6th International Conference on Information, Intelligence, Systems and Applications (IISA), 2015. DOI: 10.1109/IISA.2015.7387962

Introducing sailboats into ship routing system VISIR

Gianandrea Mannarini*, Rita Lecci, Giovanni Coppini
Ocean Predictions and Applications
Centro Euro-Mediterraneo sui Cambiamenti Climatici (CMCC)
Lecce, Italy
*)corresponding author: gianandrea.mannarini@cmcc.it

Abstract—**A prototype of sailboat routing system for least-time navigation is presented. The routing algorithm is based on an exact graph-search method, not requiring subjective optimization parameters. The temporal variation of wind fields during the sailing time is accounted for. The system also considers topological constraints such as coastline and shallow waters. The sailboat is modelled in terms of its polar plot. Wind forecasts from multiple providers are accepted as an input. Case studies show that the algorithm consistently computes tacking, jibing, and other route diversions functional to the maximum exploitation of the sailboat performance, as provided through its polar plot. The present version of the system targets races with path lengths in the range of tens of nautical miles or more.**

I. Introduction

Sailing has been traditionally linked to extensive cumulative experience, deserving also the denomination of an "art" [1]. This is nowadays still true, given the spatial and temporal variability of meteo-marine conditions and the complexity of the interaction between environment and sailboat, a consequence of the large number of degrees of freedom of the latter. However, computer-assisted decision making has been acquiring increasing weight in sailing practice for decades, due to its great potential in optimizing performance. Most active are the applications for yacht races ([2], [3]) and autonomous sailing vessels ([4], [5], [6]). An algorithm for routing of an autonomous sailboat is proposed in [4]. It is meant for short sailing in limited environments, such as lakes, where wind forecast are not existing and obstacles are not relevant. The algorithm is based on a local optimization of sailboat course, to the end of maximizing the component of velocity towards the target. In order to deal with sudden changes of wind, the width of the route corridor is constrained. The same local-optimal algorithm is part of the method by [5]. Thereto, a simplex algorithm is used, requiring the user to set the number of intermediate waypoints of the route. A second parameter controls how far from a given waypoint the route is allowed to vary. A potential field approach is used in [6], again for small robot sailboats. The potential field has the purpose of attracting the sailboat towards the target, while reproducing boat kinematics. The gradients of each of the potential components are free parameters of the method. Several commercial softwares for sailboat routing employ the isochrones method, posing however limitations in dealing with landmasses, especially in vicinity of narrow straits [7]. Our aim in this paper is to outline a coast-aware, globally optimal method for least-time sailboat routing, without making use of heuristics or subjective parameters. Furthermore, the method should be able to employ dynamic information from the forecast fields. The resulting model is designed to augment the functionalities of an already operational routing system for motorboats[1].

II. Routing algorithm

We further define the scope of our algorithm by assigning the position of a departure and an arrival mark. Also, departure time is assumed to be given, neglecting all manoeuvring needed for getting at the start line at the optimal time (see [3] for this issue). Finally, the system must work also in the coastal environment, keeping into account both the existence of obstacles (landmass) and a limited Under Keel Clearance (UKC) in shallow waters. The system must be general enough for ingesting various type of environmental forecast fields, at least wind forecast, but possibly extension to use of sea currents should be allowed. The temporal evolution of the fields should be fully exploited, as the trip or the race may last longer than the time-scale for changes of the environmental fields.

A. Graphs

In order to cope with such requirements, a graph-search algorithm is employed. A graph is a discretization of space into nodes, whereby some nodes are linked to each other. The links, or edges, define the possibility for a material point moving on the graph to travel from one node to the other. The generalized cost (e.g. elapsed time or economic expenditure) associated with such displacement is called edge weight. In a directed graph, edge weight also depends on the traveling direction [8]. We build a directed graph with nodes on a regular grid in lat/lon coordinates with spacing $1/60^o$, or about 1 NM (Nautical Mile) along the meridional (North-South) direction. Thus, races with path lengths of at least several tens of NM are within the scope of the system. Furthermore, we consider edges from each node to its first and second neighbours on the grid: This arrangement leads to an angular resolution of about 27^o [9]. For speeding up the computational time of accessing edges, the graph is represented through a forward star data structure [10]. Optimal paths on a graph minimize or maximize the sum of edge weights along the path. There are both exact and heuristics-based methods for determining such optimal paths. We here employ an exact method due to Dijkstra [11], that guarantees the global optimality of the computed path.

B. Dynamic fields

The edge weight we compute is the time needed for traversing the edge, also called "edge delay". In presence of

[1] http://www.visir-nav.com/

6th International Conference on Information, Intelligence, Systems and Applications (IISA), 2015. DOI: 10.1109/IISA.2015.7387962

dynamic environmental fields, edge delay explicitly depends on time. It can be shown that this fact results in the intuitive strategy of traversing an edge as soon as getting at one of its nodes - or First-In-First-Out (FIFO) strategy - not being always optimal and waiting times being sometimes necessary [12]. However, if edge delays do not decrease too quickly, a FIFO strategy is still optimal. Actually, the critical condition for FIFO reads: "edge delay never decreasing at a rate exceeding 100%" [12]. We make the assumption (and control it) that such rate indeed is never exceeded by the graph edges. A more sophisticated algorithmic treatment, beyond the scope of the present paper, would be required whenever this is not the case, see e.g. [13]. Therefore, we evaluate edge delays at the earliest time the edge is considered by the algorithm. Such a dynamic optimization, under the above mentioned hypothesis, has exactly the same computational complexity of a static optimization, whereby edge delays are constant in time [12].

C. Topological constraints

In order to obtain sailboat routes compliant with the topological requirements mentioned in Sect.I, the following approach is adopted. Edges intersecting or being tangent to the coastline are preliminary removed from the graph. Then, once the actual sailboat class is specified, the remaining edges are further screened for the condition that UKC $= z - T > 0$, where z is mean sea depth along a given edge and T is the sail-class-specific draught. The procedure is fully equivalent to the one for the computation of the "safegram", illustrated in [9]. Finally, the route optimization algorithm (Dijkstra) is run on the graph subset containing just topologically safe edges. Both coastline and bathymetry are parts of NOAA datasets: [14], [15].

III. Sailboat modelling

Modelling of the sailboat performance is challenging. Hydrodynamic modelling of hull-water interaction has to be combined with sail aerodynamics and stability constraints. Numerical models accounting for these effects are called in sailboat jargon Velocity Prediction Programs (VPPs) [16]. In VPPs many dynamical aspects are parametrized, based on towing tank and wind tunnel measurements [17]. The typical output of a VPP is a sailboat response function, usually plotted in the form of a polar plot as sustained sailboat speed vs. point of sail, for various values of wind intensity. There are 2 alternative viewpoints for representing this information: the moving sailboat and a stationary observer on the land. Adopting the latter, the angle between sailboat course and wind direction or True Wind Angle (TWA) and the True Wind Speed (TWS) are considered. These are the independent variables in the plots of Fig.1a-d. Sustained speed is non-null even for some upwind directions, thanks to the lift on the sail. However, for closer and closer hauled sailing points (TWA$\sim 30^o$), a no-go-zone is reached, whereby no upwind motion is possible. For an introduction to these topics, see [18]. The most performing point of sail depends on the projection $v \cdot |\cos(\mathrm{TWA})|$ of boat speed v on the upwind or downwind direction. Optimal values of such "Velocity Made Good" (VMG) are shown in Fig.1a-c for different TWS. While a polar plot tends to highlight the angular dependence on sailboat response function, the nonlinear dependance on TWS is more easily recognized via plots such as those of Fig.1(b,d). Furthermore, the wind force results in a heeling moment on the sailboat, eventually causing a leeway drift. This information is sometimes present in a polar plot [19]. Typical leeway angle is usually much smaller (0-6 deg) than the minimum angle resolved in the graph used in this work ($\sim$27 deg, see Sect.II). Thus, it is not critical for our application to neglect it, as we do. Other approximations here done include: not accounting for ocean currents and tidal currents (they could play a role in presence of weak wind), neglecting beat tack time (a few seconds vs. typical route duration gains in range of minutes, see Tab.II), use of a fixed sail/polar plot.

TABLE I. Sailboat parameters

Class	Parameter	Symbol	Value	Units	Source
First 36.7	Draught	T	2.1	m	[21]
	Length over all	L	11.0	m	
J24	Draught	T	1.2	m	[22]
	Length over all	L	7.3	m	

IV. Wind forecast data

The sailboat mast can be as high as two times the hull length. Thus, the wind shear (intensity and directional variation) between boom and masthead height may be noticeable. This effect (twist) is neglected in this paper and the routing system is fed through wind forecast fields at 10m height. Relevant features of the forecast fields used are discussed below.

A. Forecast models

In this paper we employ 10m wind forecast from IFS model (Cy40r1) operated by the European Centre for Medium-Range Weather Forecasts (ECMWF) [23] and 10m wind forecast from COSMO-ME model operated by Centro Nazionale di Meteorologia e Climatologia Aeronautica (CNMCA) [24]. COSMO-ME receives IFS model outputs as lateral boundary conditions. For both models, we consider forecast fields relative to the analysis carried out at 12:00 UTC. Both forecast model outputs are available with 3-hourly resolution for the first 3 days after the analysis. IFS forecast fields at 2 different horizontal resolutions, 1/4^o (15 NM) and 1/8^o (7.5 NM), and COSMO-ME at the resolution of 1/16^o (3.75 NM) are used in this work.

B. Forecast verification

IFS products undergo routine verification vs. observations [25]. In particular, IFS 10m wind over ocean showed in the period September 2012 - August 2013 a scatter index (standard deviation of error normalised by the mean observed value) between 15% and 30% during the first 3 days after analysis. Wavenumber spectral analysis shows that ECMWF model underestimates synoptic and mesoscale wind intensity vs. altimeter observations, see [27] for Mediterranean Sea data. For COSMO-ME some information about verification is available on [26]. Using 2011-2012 observations, a mean absolute error below 1 kts and a root mean square error below 1.5 kts are found. These error metrics are rather independent of forecast step and are comparable if not better than IFS scores on the same stations.

6th International Conference on Information, Intelligence, Systems and Applications (IISA), 2015. DOI: 10.1109/IISA.2015.7387962

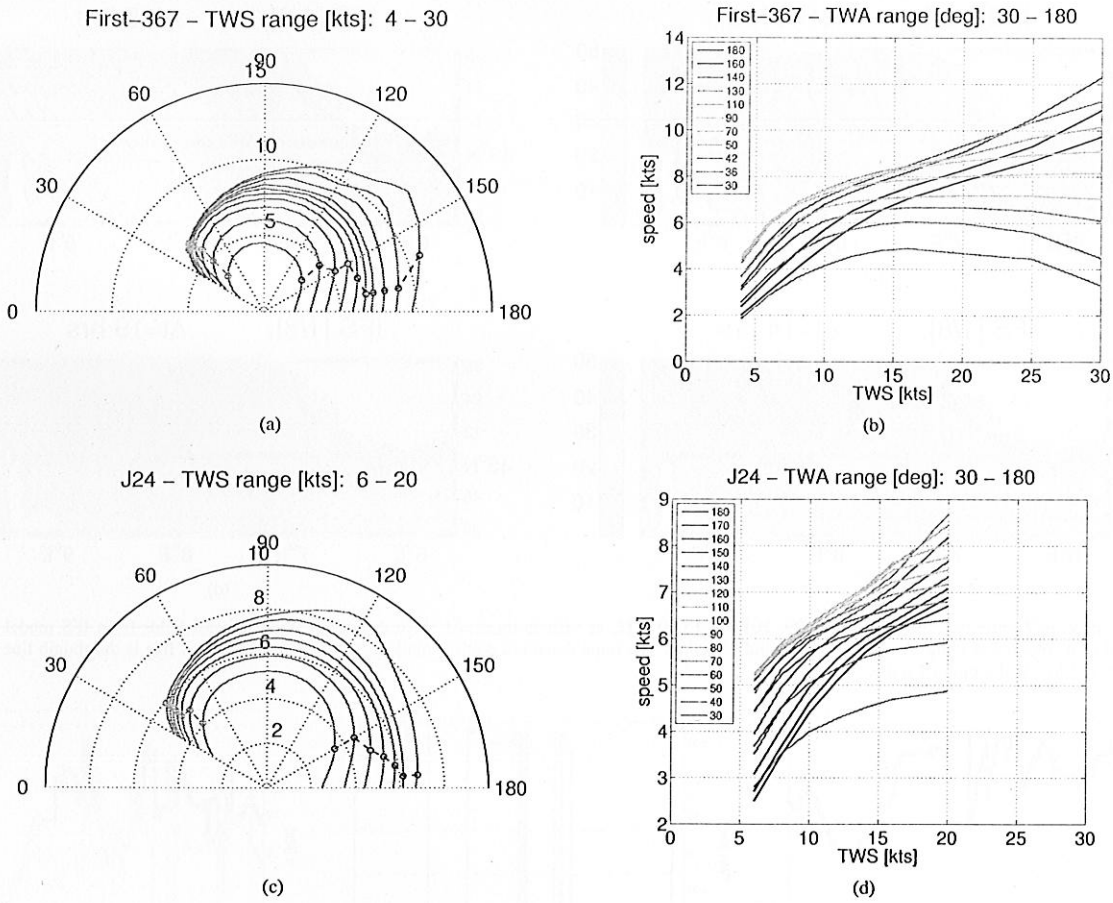

Fig. 1. Sailboat response function for a First 36.7 (a,b) and a J24 sailboat (c,d). In polar plots (a,c), the sailboat speed is displayed along the radial coordinate vs. TWA along the azimuthal coordinate, for various TWS values (blue lines). Note the different radial range for a) and c) panels. The magenta and black dashed lines with dots denote respectively the upwind and downwind optimal point of sail, based on VMG. In (b,d) panels the same information is plotted vs. TWS, for a selection of TWAs from the corresponding (a,c) panels. Polar plot source data of the two sailboats are obtained from [19] and [20].

V. Case Studies

In order to demonstrate the potential of the method described in Sect.II-IV, we consider two case studies in the Mediterranean Sea. One of them (Sect.V-A) is a route with prevailing downwind and the other one (Sect.V-B) with prevailing upwind sailing conditions. We note that, given the no-go-zone and the limiting values for TWS in the polar plot of any sailboat, a route between assigned end-points may not exist for any departure time. In the present work, the FIFO condition of Sect.II-B is checked for at each time step of the forecast fields. It turns out that FIFO is always fulfilled in the cases considered. Also, the Velocity-Made-good to Course (VMC) is computed along the routes. VMC is defined as the projection of sailboat speed onto the instantaneous direction to the target mark. VMC is positive (negative) if the sailboat is approaching (going away from) the target. In the case studies below, both snapshots of the forecast fields with the cumulative route up to a given time Δt since departure, and the full time evolution of selected fields along the route vs. Δt are displayed.

A. Route: Toulon - Corsica

In this case, a First 36.7 is sailed downwind in presence of a Beaufort 7 westerly wind. From Fig.2(a-d) it is seen that the wind reaches gale intensity at about Δt=9 hrs and then falls. The algorithm is able to fully exploit such a dynamic information. In fact, the optimal route diverts northwards by several tens of nautical miles before getting to destination. The sequence of frames shows that, after gale intensity winds are skipped (a,b), the route approaches the rhumb line route at the time the gale withdraws southwards (c). Inspection of TWS experienced along the route (Fig.3a) reveals that jibing is required (Fig.3b) as TWS approaches the limit of 30 kts set by the polar plot (Fig.1b) for this specific boat. At those locations, the boat jibs at about TWA=160°, being close to the the optimal downwind point of sail, according to the polar plot of Fig.1a. As a result, a speed close to top value 12 kts is sustained during this route, as seen from Fig.3c. It is also seen that the northbound diversion (peaking at Δt=6.4 hrs since departure) is paid at the highest price in terms of VMC, falling to less than 6 kts. However, for the given departure date and time, constraining a more limited northbound manoeuvring would lead to no route at all (not shown).

6th International Conference on Information, Intelligence, Systems and Applications (IISA), 2015. DOI: 10.1109/IISA.2015.7387962

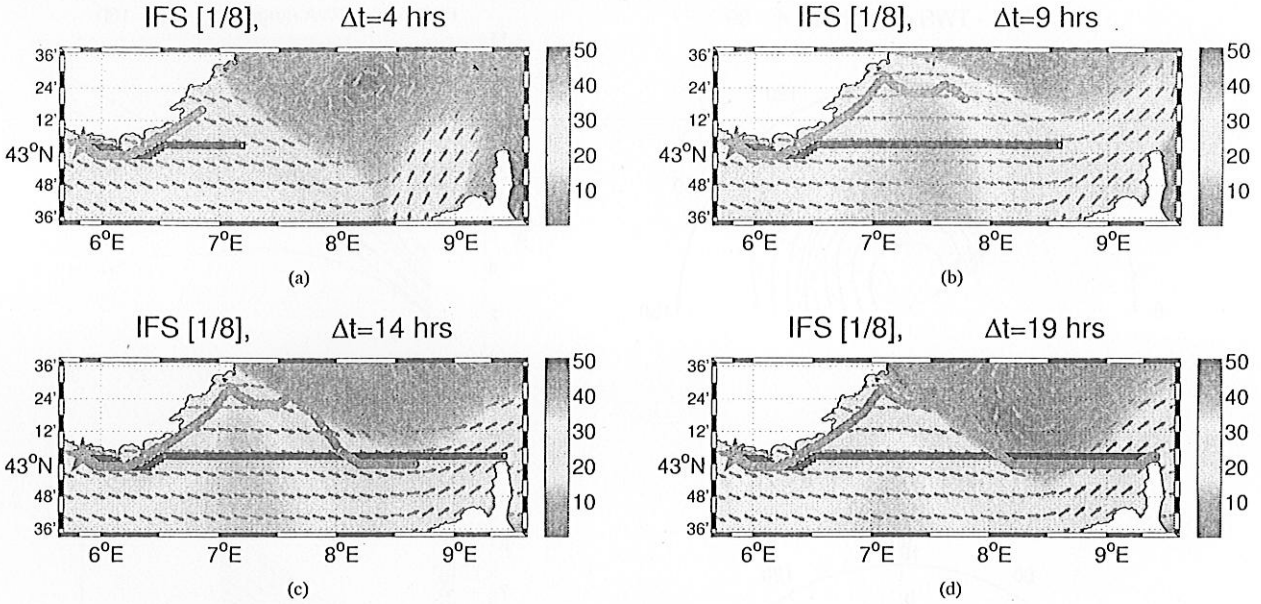

Fig. 2. First 36.7 route departing on March 29, 2015 at 15:00 UTC at various times Δt since departure. Wind forecast fields from IFS model at 1/8° are displayed as a coloured shading. Arrows indicate wind direction. The route departure point is marked by a red star. The black line is the rhumb line or geodetic route; the red line is the optimal route.

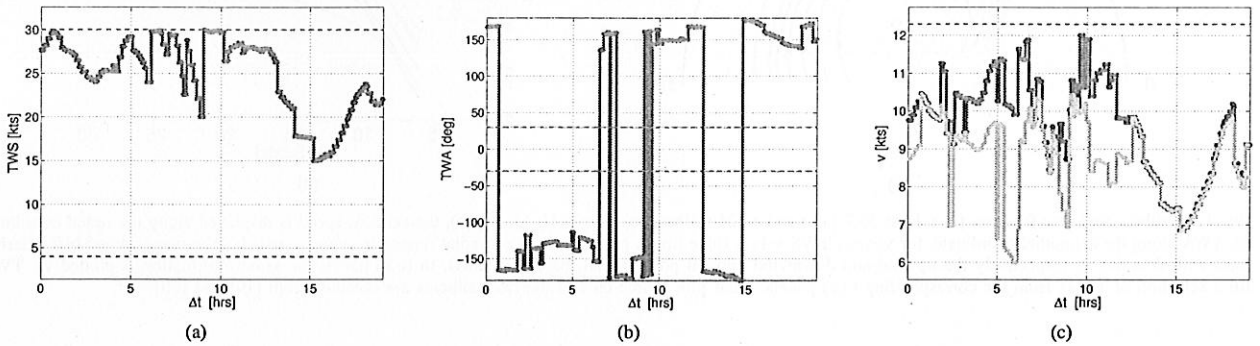

Fig. 3. Information along the optimal route of Fig.2. TWS (red line) and TWS extrema according to the polar plot (blue dashed lines) are displayed in panel (a). TWA in degrees (red line) and dashed lines delimiting the no-go-zone of Fig.1a are displayed in panel (b). Sailboat speed (red line), VMC (green line), and sailboat top speed (blue dashed line) according to its polar plot are displayed in panel (c).

B. Route: Stromboli - Marina di Caronia

In this case, routes under prevailing upwind conditions are computed (Fig.4, Fig.5). Wind intensity is in the moderate to fresh breeze range (Beaufort 4-5). The geodetic route passes between Lipari and Salina, in the Eolie islands. The sea can be very deep in this portion of the Thyrrenian Sea, but close to the shelf of Sicily, Fig.4e. The effect of using a J24 sailboat and forecast fields from respectively IFS 1/4°, IFS 1/8°, COSMO-ME 1/16° is compared in Fig.4a-c and Fig.5a-f. While both IFS model outputs lead to an optimal route passing through Salina and Filicudi and then northern of Alicudi, use of the COSMO-ME output leads to a route passing North of Filicudi. The first two routes (IFS forecast) require tacking at about Δt=6 hrs and Δt=9 hrs, experiencing even a negative VMC and cumulating a significant cross-track error in the close hauled phase. Afterwards, a broad reach phase is computed by the algorithm, see Fig.5a,b,d,e. The COSMO-ME route instead (Fig.4c) is completely upwind, implying just two tackings, and VMC$<$ 0 for a more limited time period at about Δt=8.3 hrs (Fig.5c). Mainly thanks to a stronger wind forecast for $\Delta t \geq$13 hrs (not shown), the COSMO-ME one is the fastest of the three routes, see Tab.II. If the COSMO-ME forecast is used in combination with a First 36.7 and not J24 polar plot, destination is reached after 4 tackings (though the latter 2, occurring at Δt=6.5 hrs as the route approaches the coast of Sicily for the first time, are hardly noticed in the map of Fig.4d). Finally, if again a J24 and COSMO-ME are used, but the spatial domain for route optimization is constrained to the West as in Fig.4f, a geometrically shorter route is indeed computed, Tab.II. However, such a shorter route lasts nearly 9 minutes more than the unconstrained one in Fig.4c. At a speed of 6 kts, this means being still about 1 NM far from the finish line, as a competing boat sailing on the route resulting from the unconstrained algorithm wins the race.

6th International Conference on Information, Intelligence, Systems and Applications (IISA), 2015. DOI: 10.1109/IISA.2015.7387962

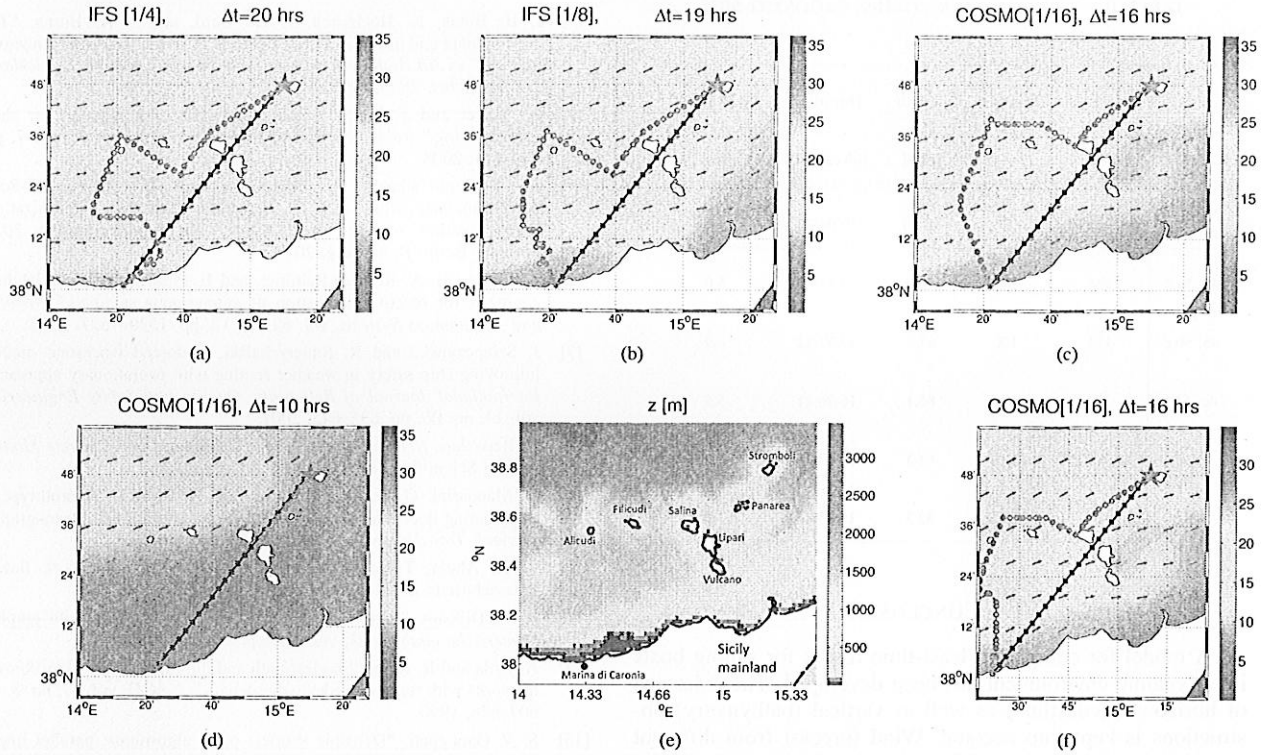

Fig. 4. Route departing on March 29, 2015 at 15:00 UTC, displayed at the time step at which the target is reached. The route departure point is marked by a red star. A J24 sailboat and forecasts from IFS 1/4, IFS 1/8 and COSMO-ME 1/16 are employed respectively in panels (a,b,c). In panel (d) a First 36.7 and COSMO-ME 1/16 forecasts are used. Panel (e) displays the bathymetry of the domain. In panel (f), everything as in panel (c) but the western extent of the buffer zone for the route optimization.

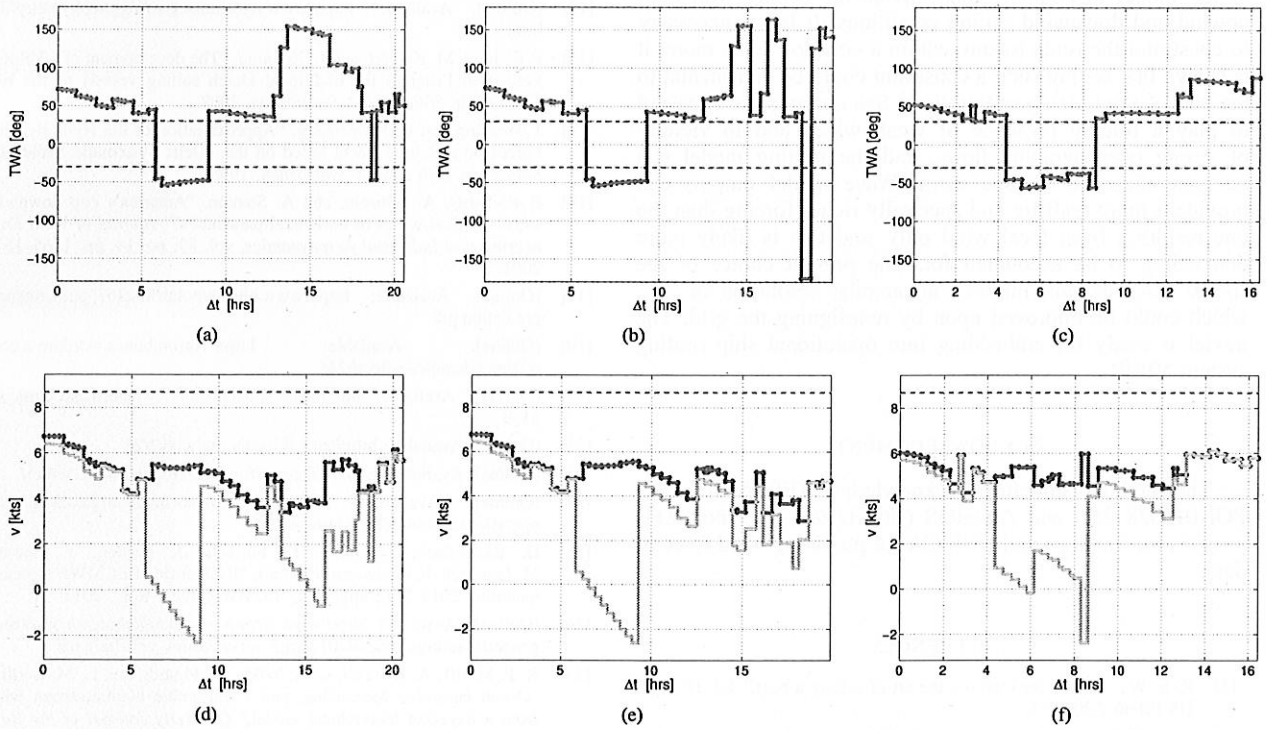

Fig. 5. Each column contains information along the optimal routes of Fig.4(a-c) respectively. In the upper row, TWA (red lines) and no-go-zone (blue dashed lines); In the lower row, sailboat speed (red lines), VMC (green lines), and sailboat top speed (blue dashed lines) are displayed.

6th International Conference on Information, Intelligence, Systems and Applications (IISA), 2015. DOI: 10.1109/IISA.2015.7387962

TABLE II. ROUTE METRICS (I=IFS, C=COSMO-ME)

Fig.	Class	Forecast	Length [NM]	Duration [hh:mm:ss]	Mean speed [kts]
2-3	First 36.7	I/8	184.0	19:04:36	9.6
4a, 5a,d	J24	I/4	103.1	20:33:52	5.0
4b, 5b,e	J24	I/8	97.2	19:52:22	4.9
4c, 5c,f	J24	C/16	86.1	16:26:21	5.2
4d	First 36.7	C/16	64.5	10:17:28	6.3
4f	J24	C/16	82.5	16:35:16	5.0

VI. CONCLUSION

A model for computing least-time routes for sailing boats in a dynamic environment has been developed. The existence of horizontal (coastline) as well as vertical (bathymetry) obstructions is kept into account. Wind forecast from different providers can be employed. Sailboat class can be adjusted by providing corresponding polar plot. The model is based on an exact optimization algorithm, not requiring subjective parameters or heuristic functions. Case studies show the capacity of the model to compute manoeuvres for coping with both upwind and downwind sailing conditions. It is not necessary to constraint the route to stay within a corridor. Even more, it is shown that setting such a constraint could be detrimental to the aim of minimizing sailing time. Sea currents are expected to play a role in presence of weak winds and in vicinity of strong oceanographic flows, and the routing model can be generalized to include them. Wave model outputs can provide a more realistic and spectrally richer forcing than the one resulting from local wind only, and this is likely more demanding to be accounted for. The present choice of the spatial discretization imposes an angular resolution of 27^o, which could be improved upon by redesigning the grid. The model is ready for embedding into operational ship routing system VISIR.

ACKNOWLEDGMENT

The authors gratefully acknowledge TESSA (contract PON01_02823/2) and AtlantOS (EC-H2020 grant #633211) projects for fundings and CNMCA for providing wind forecast data.

REFERENCES

[1] R. S. W., "Device for teaching the art of sailing a boat," Jul. 16 1940, US Patent 2,208,083.

[2] A. B. Philpott, S. Henderson, and D. Teirney, "A simulation model for predicting yacht match race outcomes," *Operations Research*, vol. 52, no. 1, pp. 1–16, 2004.

[3] J. R. Binns, K. Hochkirch, F. De Bord, and I. A. Burns, "The development and use of sailing simulation for IACC starting manoeuvre training," in *3rd High Performance Yacht Design Conference, Auckland, 2-4 December, 2008*, 2008.

[4] R. Stelzer and T. Pröll, "Autonomous sailboat navigation for short course racing," *Robotics and autonomous systems*, vol. 56, no. 7, pp. 604–614, 2008.

[5] J. Cabrera-Gámez, J. Isern-González, D. Hernández-Sosa, A. Domínguez-Brito, and E. Fernández-Perdomo, "Optimization-based weather routing for sailboats," in *Robotic Sailing 2012*. Springer Berlin Heidelberg, 2013.

[6] C. Pêtrès, M.-A. Romero-Ramirez, and F. Plumet, "A potential field approach for reactive navigation of autonomous sailboats," *Robotics and Autonomous Systems*, vol. 60, no. 12, pp. 1520–1527, 2012.

[7] J. Szlapczynska and R. Smierzchalski, "Adopted isochrone method improving ship safety in weather routing with evolutionary approach," *International Journal of Reliability, Quality and Safety Engineering*, vol. 14, no. 06, pp. 635–645, 2007.

[8] D. Bertsekas, *Network Optimization: Continuous and Discrete Models*. Athena Scientific, 1998.

[9] G. Mannarini, G. Coppini, P. Oddo, and N. Pinardi, "A prototype of ship routing decision support system for an operational oceanographic service," *TransNav*, vol. 7, no. 1, pp. 53–59, 2013.

[10] R. K. Ahuja, T. L. Magnanti, and J. B. Orlin, "Network flows," Massachusetts Institute of Technology, Tech. Rep., 1988.

[11] E. W. Dijkstra, "A note on two problems in connexion with graphs," *Numerische mathematik*, vol. 1.1, pp. 269–271, 1959.

[12] A. Orda and R. Rom, "Shortest-path and minimum-delay algorithms in networks with time-dependent edge-length," *J. ACM*, vol. 37, no. 3, pp. 607–625, 1990.

[13] S. V. Ganugpati, "Dynamic shortest paths algorithms: parallel implementations and application to the solution of dynamic traffic assignment models," Ph.D. dissertation, Massachusetts Institute of Technology, 1998.

[14] [Online]. Available: http://www.ngdc.noaa.gov/mgg/shorelines/gshhs.html

[15] [Online]. Available: http://www.ngdc.noaa.gov/mgg/bathymetry/iho.html

[16] P. de Jong, M. Katgert, and L. Keuning, "The development of a Velocity Prediction Program for traditional Dutch sailing vessels of the type Skûtsje," in *20th HISWA Symposium*, 2008.

[17] J. Keuning and U. Sonnenberg, "Approximation of the Hydrodynamic Forces on a Sailing Yacht based on the. 'Delft Systematic Yacht Hull Series," in *15th HISWA Symposium*, 1998.

[18] P. Richards, A. Johnson, and A. Stanton, "America's cup downwind sails—vertical wings or horizontal parachutes?" *Journal of Wind Engineering and Industrial Aerodynamics*, vol. 89, no. 14, pp. 1565–1577, 2001.

[19] [Online]. Available: http://www.blur.se/polar/first367_performance_prediction.pdf

[20] [Online]. Available: http://76trombones.wordpress.com/offshore-handicap-fleet/j24/

[21] [Online]. Available: http://sailboatdata.com/viewrecord.asp?class_id=3159

[22] [Online]. Available: http://en.wikipedia.org/wiki/J/24

[23] [Online]. Available: http://old.ecmwf.int/research/ifsdocs/CY40r1/

[24] [Online]. Available: http://www2.cosmo-model.org/content/tasks/operational/usam/default.htm#setup

[25] D. Richardson, J. Bidlot, L. Ferranti, T. Haiden, T. Hewson, M. Janousek, F. Prates, and F. Vitart, "Evaluation of ECMWF forecasts, including 2012-2013 upgrades," ECMWF, Tech. Rep., 2013.

[26] [Online]. Available: http://www.cosmo-model.org/content/consortium/generalMeetings/general2012/wg5-versus/tesini_verifItaly.pdf

[27] R. F. Milliff, A. Bonazzi, C. K. Wikle, N. Pinardi, and L. M. Berliner, "Ocean ensemble forecasting. part i: Ensemble mediterranean winds from a bayesian hierarchical model," *Quarterly Journal of the Royal Meteorological Society*, vol. 137, no. 657, pp. 858–878, 2011.